Heat Mass Transfer (2012) 48:799–807
DOI 10.1007/s00231-011-0937-y

ORIGINAL

# The effect of material properties on the performance of a new geometry PEM fuel cell

**Iman Khazaee · Mohsen Ghazikhani**

Received: 21 April 2011 / Accepted: 3 November 2011 / Published online: 15 November 2011


**Abstract** In this paper a computational dynamics model for duct-shaped geometry proton exchange membrane (PEM) fuel cell was used to investigate the effect of changing gas diffusion layer and membrane properties on the performances, current density and gas concentration. The proposed model is a full cell model, which includes all the parts of the PEM fuel cell, flow channels, gas diffusion electrodes, catalyst layers and the membrane. Coupled transport and electrochemical kinetics equations are solved in a single domain; therefore no interfacial boundary condition is required at the internal boundaries between cell components. This computational fluid dynamics code is used as the direct problem solver, which is used to simulate the 2-dimensional mass, momentum and species transport phenomena as well as the electron- and proton-transfer process taking place in a PEMFC that cannot be investigated experimentally. The results show that by increasing the thickness and decreasing the porosity of GDL the performance of the cell enhances that it is different with planner PEM fuel cell. Also the results show that by increasing the thermal conductivity of the GDL and membrane, the overall cell performance increases.

**List of symbols**

$A$ Superficial electrode Area, $m^2$
$C$ Molar concentration, $mol/m^3$
$D$ Species diffusivity, $m^2/s$
$I$ Current density, $A/m^2$
$i_0$ Reference current density, $A/cm^2$
$U$ Inlet velocity, m/s
$j$ Transfer current density, $A/m^3$
$\vec{u}$ Velocity vector, m/s
$p$ Pressure, Pa
$S$ Stoichiometric ratio
$T$ Temperature, K

**Greek letters**

$\eta$ Overpotential, V
$\rho$ Density, $kg/m^3$
$\varepsilon$ Porosity
$\sigma$ Ionic conductivity, S/m
$\phi$ Phase potential, V
$v$ Volumetric flow rate, $m^3/s$
$\xi$ Water content of the membrane
$\mu$ Viscosity, kg m/s
$\alpha$ Transfer coefficient for the reaction

I. Khazaee (✉)
Department of Mechanical Engineering, Torbat-e-jam Branch, Islamic Azad University, Torbat-e-jam, Iran
e-mail: imankhazaee@yahoo.com

M. Ghazikhani
Department of Mechanical Engineering, Faculty of Engineering, Ferdowsi University of Mashhad, P.O. Box 9177948944-1111, Mashhad, Iran

## 1 Introduction

A fuel cell is an electro-chemical energy device that converts the chemical energy of fuel directly into electricity and heat, with water as a by-product of the reaction. Based on the types of electrolytes used, they are categorized into polymer electrolyte membrane fuel cells (PEMFCs), solid oxide fuel cells (SOFCs), phosphoric acid fuel cells (PAFCs), molten carbonate fuel cells (MCFCs), and direct methanol fuel cells (DMFCs). The polymer exchange membrane fuel cell (PEMFC) is considered to be the most promising candidate for electric vehicles by virtue of its

high power density, zero pollution, low operating temperature, quick start-up capability and long lifetime. PEMFC can also be used in distributed power systems, submarines, and aerospace applications as discussed by Larminie and Dicks [1].

The single-cell PEMFC consists of a carbon plate, a gas diffusion layer (GDL), a catalyst layer, for each of the anode and the cathode sides, as well as a PEM membrane at the center.

Flow channel geometry is of critical importance for the performance of fuel cells containing proton exchange membranes (PEM) but is of less concern for solid oxide fuel cells (SOFC). The reactants, as well as the products, are transported to and from the cell through flow channels. Flow field configurations, including parallel, serpentine, interdigitated, and other combined versions, have been developed.

The performance of the fuel cell system is characterized by current–voltage curve (*i.e. polarization curve*). The difference between the open circuit potential of the electrochemical reaction and cell voltage occurs from the losses associated with the operation. The corresponding voltage drop is generally classified in three parts:

1. activation over-potential caused by the electrochemical reactions,
2. ohmic drop across the polymer electrolyte
3. mass transfer limitations of reactants

These associated losses dominate over different current density ranges. For low current densities; the activation over-potential is dominant. For high current densities, which are of particular interest for vehicle applications because of higher power density; the mass transfer limitations dominates the losses. For moderate current densities, the ohmic drop across the polymer membrane dominates. Moreover, for high current densities, water starts to exist in liquid form leading to a two-phase transport of reactants to reaction site, which is an additional transport phenomenon of PEM fuel cell operation.

Khazaee and Ghazikhani [2] proposed a complete 3-dimensional and single phase model for annular-shaped proton exchange membrane (PEM) fuel cell to investigate the effect of using different connections between bipolar plate and gas diffusion layer on the performances, current density, and temperature and gas concentration. They found that that the cell performance is increased as the number of connections between GDL and bipolar plate increases but for one connection conditions the effect of changing the location of connection on cell performance is negligibly small. Also they found that the water mole fraction gradually increases along the cell and the maximum of it is near the connections between GDL and bipolar plate.

West and Fuller [3] proposed a 2-dimensional numerical analysis of the rib spacing in PEM electrode assemblies on current and water distribution within the cell. The results indicated that increasing the rib width strongly affected the membrane water content before the catalyst utilization is reduced. Therefore, the 2-dimensional effect has a significant influence on water management.

Chiang and Chu [4] investigated the effects of transport components on the transport phenomena and performance of PEM fuel cells by using a 3-dimensional model. The impacts of channel aspect ratio (AR) and GDL thickness were examined. It was found that a flat channel with a small AR or a thin GDL generates more current at low cell voltage due to the merits of better reactant gas transport and liquid water delivery.

Wang et al. [5] developed a 2-dimensional numerical model to study the two-phase flow transport in the air cathode of a PEMFC. In this paper, the model encompassed both single- and two-phase regimes corresponding to low and high current densities and was capable of predicting the transition between the two regimes.

Kuo et al. [6] performed numerical simulations to evaluate the convective heat transfer performance and velocity flow characteristics of the gas flow channel design to enhance the performance of proton exchange membrane fuel cells (PEMFCs). Their study has simulated low Reynolds number laminar flow in the gas flow channel of a PEMFC. The heat transfer performance and enhanced gas flow velocity characteristics of four different channel geometries have been considered, namely a conventional straight gas flow channel and a gas flow channel with the three novel periodic patterns geometries. The results indicated that, compared to the conventional gas flow channel, the novel gas flow channels proposed in this study provide a significantly improved convective heat transfer performance and a higher gas flow velocity and, hence, an improved catalysis reaction performance in the catalyst layer.

Yan et al. [7] developed a 2-dimensional mass transport model to investigate the anode gas flow channel cross section and GDL porosity effects. They found that an increase in either the GDL porosity, channel width fraction, or the number of channels could lead to better cell performance.

Chu et al. [8] also used a half-cell model to investigate the effect of the change of the GDL on the performance of a PEMFC. They found that a fuel cell embedded with a GDL with a larger averaged porosity will consume a greater amount of oxygen, so that a higher current density is generated and a better fuel cell performance is obtained.

In this work a 3-dimensional and single phase CFD model for duct-shaped geometry with four connections of a proton exchange membrane (PEM) fuel cell is presented to investigate the effect of changing material properties of the

membrane and gas diffusion layer on the performance, current density and gas concentration. The objective of the current work is to show using a different geometry of the fuel cell and the effect of changing the thickness, porosity and thermal conductivity of the GDL and membrane that it may be of interest to engineers attempting to develop the optimization of a PEMFC and to researchers interested in the flow modification aspects of the PEMFC performance enhancement.

## 2 Numerical model

The cathode electrochemical reactions produce a large amount of liquid water at low operating voltages. If the liquid water is not properly removed and accumulates in the pores of the porous layers, it restricts the oxygen transport to the gas diffusion layer and the catalyst layer, thereby reducing the electrochemical reaction rate.

The numerical model for the fuel cell used here includes the anode flow channels, anode gas diffusion layer, anode catalyst layer, proton exchange membrane, cathode catalyst layer, cathode gas diffusion layer, and cathode flow channels. The model of this study is similar to the model that was used in the previous work [2] that is a new geometry in fuel cell field. Miniature duct-shaped fuel cell with dimensions of 4.512 mm × 4.512 mm × 12 mm is considered in this investigation. The gas diffusion layer is 0.3 mm thick, the catalyst layer is 0.01 mm thick, and the proton exchange membrane is 0.05 mm thick.

The physical problem considered in this paper is the 3-dimensional cell model of the PEMFC system as shown in Fig. 1.

The proposed model does not require any internal boundary conditions between the components of PEM fuel cell system [2]. The difference between this model and another model is the utilization of it to closed geometries like the annular geometry and duct-shaped geometry in comparison of a fuel cell with planner geometry. The different physical properties and transport parameters are incorporated into a single set of governing equations using a single domain formulation. The model aims to study the electrochemical kinetics, current distribution, reactant flow fields and multi-component transport of oxidizer and fuel streams in a multi-dimensional domain. The assumptions made in developing the model are as follows:

Ideal gas mixtures
Incompressible and Laminar flow because low flow velocities and low fuel utilization
Isotropic and homogeneous porous electrodes, catalyst layers and membrane
Negligible ohmic resistance at porous electrodes and current collectors

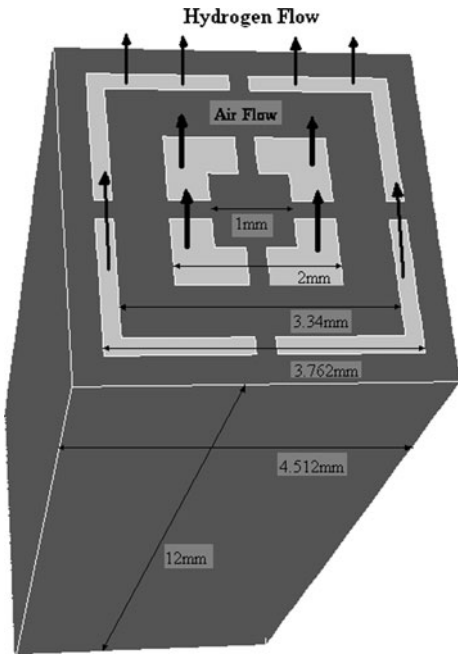


**Fig. 1** Computational domain and schematic of duct-shaped PEMFC with four connections

The model assumes that the system is steady; the inlet reactants are ideal gases; the flow is laminar; and the porous layers such as the diffusion layer, catalyst layer and PEM are isotropic. The model includes continuity, momentum and species equations for gaseous species, liquid water transport equations in the channels, gas diffusion layers, and catalyst layers, water transport equation in the membrane, electron and proton transport equations. The Bulter–Volumer equation was used to describe electrochemical reactions in the catalyst layers.

The conservation equations of mass, momentum, energy, species and charge are as follows:

$$\frac{\partial(\rho\varepsilon)}{\partial t} + \nabla\cdot(\varepsilon\rho\vec{u}) = 0 \tag{1}$$

$$\frac{\partial(\rho\varepsilon\vec{u})}{\partial t} + \nabla\cdot(\varepsilon\rho\vec{u}\vec{u}) = -\varepsilon\nabla p + \nabla\cdot(\varepsilon\mu\nabla\vec{u}) + S_u \tag{2}$$

$$\frac{\partial(\rho\vec{u}(E+p))}{\partial t} + \nabla\cdot((E+p)\rho\vec{u}\vec{u}) = \nabla\cdot\left(\lambda_{\text{eff}}\nabla T - \sum_k h_k J_k + (\tau_{\text{eff}}\cdot\vec{u})\right) + S_h \tag{3}$$

$$\frac{\partial(\varepsilon X_k)}{\partial t} + \nabla\cdot(\varepsilon\vec{u}X_k) = \nabla\cdot\left(D_k^{\text{eff}}\nabla X_k\right) + S_k \tag{4}$$

$$\nabla\cdot\left(\sigma_g^{\text{eff}}\nabla\phi_e\right) + S_\phi = 0 \tag{5}$$

where $\vec{u}, X_k, h_k, \tau_{\text{eff}}\lambda_{\text{eff}}$ and $\phi_e$ denotes intrinsic velocity vector, molar fraction of $k$th species, enthalpy of species $k$, effective stress tensor which can be ignored due to the low

velocity of laminar gas flow, effective thermal conductivity in a porous material consisting of the electrode solid matrix and gas and electrolyte phase potential, respectively. The corresponding source terms treating the electrochemical reactions and porous media are presented in Table 1.

$$\lambda_{\text{eff}} = \varepsilon\lambda_f + (1-\varepsilon)\lambda_s \tag{6}$$

where $\lambda_s$ is the thermal conductivity of the electrode solid matrix and $\lambda_f$ is the thermal conductivity of the gas, which can be expressed as a function of temperature:

$$\lambda_f = a_0 + a_1 T + a_2 T^2 + a_3 T^3 \tag{7}$$

It is of benefit to further explain the corresponding diffusivities of the governing equations. The diffusivities for species concentration equations and ionic conductivity for membrane phase potential equation are modified using Bruggman correlation to account for porous electrodes, which can be expressed as:

$$D_k^{\text{eff}} = \varepsilon_m^{1.5} D_k \tag{8}$$

$$\sigma_e^{\text{eff}} = \varepsilon_m^{1.5} \sigma_e \tag{9}$$

It is worth further explaining the mole fraction of oxygen appearing in Eq. 4 because oxygen is a gaseous species in the cathode flow channel and gas-diffusion electrode but becomes a species dissolved in the electrolyte in the catalyst layer and membrane regions. Our definition is given by

$$X_k = \begin{cases} C_k^g / C_{\text{tot}} & \text{in gas} \\ C_k^e / C_{\text{tot}} & \text{in electrode} \end{cases} \tag{10}$$

where $C_k$ is the molar concentration of species $k$ and superscripts $g$ and $e$ denote the gas and the electrolyte phases, respectively. Thus, $X_k$ is a true mole fraction in the gas phase but is a pseudo mole fraction when species $k$ is in the dissolved form. In addition, there is a discontinuity in the value of $X_k$ at the interface between the gas-diffusion electrode and the catalyst layer due to the following thermodynamic relation

$$C_k^{e,\text{sat}} = \frac{RT}{H} C_k^g \tag{11}$$

where $H$ is the Henry's law constant equal to $2 \times 10^5$ atm cm$^3$/mol for oxygen in the membrane.

Either generation or consumption of chemical species $k$ and the creation of electric current occurs only in the active catalyst layers where electrochemical reactions take place. The $S_k$ and $S_\phi$ terms are therefore related to the transfer current between the solid matrix and the membrane phase inside each of the catalyst layers. These transfer currents at anode and cathode can be expressed as follows

$$j_a = a j_{0,a}^{\text{ref}} \left( \frac{X_{\text{H}_2}}{X_{\text{H}_2,\text{ref}}} \right)^{1/2} \left( \frac{\alpha_a + \alpha_c}{RT} \cdot F \cdot \eta \right) \tag{12}$$

$$j_c = -a j_{0,c}^{\text{ref}} \left( \frac{X_{O_2}}{X_{\text{O}_2,\text{ref}}} \right)^{1/2} \left( -\frac{\alpha_c \cdot F}{RT} \cdot \eta \right) \tag{13}$$

the above kinetics expressions are derived from the general Bulter-Volmer equation based on the facts that the anode exhibits fast electrokinetics and hence a low surface overpotential to justify a linear kinetic rate equation, and that the cathode has relatively slow kinetics to be adequately described by the Tafel equation. In Eqs. 12 and 13, the surface overpotential, $\eta(x, y)$, is defined as

$$\eta(x,y) = \phi_s - \phi_e - V_{\text{oc}} \tag{14}$$

where $\phi_s$ and $\phi_e$ stand for the potentials of the electronically conductive solid matrix and electrolyte, respectively, at the electrode electrolyte interface. $V_{\text{oc}}$ is the reference open-circuit potential of an electrode. It is equal to zero on the anode but is a function of temperature on the cathode namely

$$V_{\text{oc}} = 0.0025T + 0.2329 \tag{15}$$

**Table 1** Source terms

| | $S_v$ (momentum) | $S_k$ (species) | $S_\phi$ (phase potential) | $S_n$ (energy) |
|---|---|---|---|---|
| Gas channels | 0 | 0 | 0 | 0 |
| Backing layers | $\frac{-\mu}{k}\varepsilon^2\vec{u}$ | 0 | 0 | 0 |
| Catalyst layers | $\frac{-\mu}{k}\varepsilon^2\vec{u}$ | $-\frac{j_a}{2F}\frac{\rho}{\varepsilon_m\varepsilon_{mc}}$: anode $H_2$<br>$\frac{j_c}{2F}\frac{\rho}{\varepsilon_m\varepsilon_{mc}}$: cathode $O_2$<br>$-\frac{j_c}{F}\left(\frac{1}{2}+n_d\right)\frac{\rho}{\varepsilon_m\varepsilon_{mc}}$: cathode $H_2O$<br>$-\frac{n_d}{F}j_a\frac{\rho}{\varepsilon_m\varepsilon_{mc}}$: anode $H_2O$ | $j$ | $\frac{\lvert j_c\rvert}{2F}T\lvert\Delta s\rvert + \lvert j_c\eta_c\rvert$ For cathode<br>0 For anode |
| Membrane | $\frac{-\mu}{k}\varepsilon^2\vec{u}$ | 0 | 0 | $\frac{I^2}{K_{\text{mem}}}$ |

where $T$ is in Kelvin and $V_{oc}$ is in volts. Notice that $V_{oc}$ is not the true open-circuit potential of an electrode, which would then depend upon reactant concentrations according to the Nernst equation.

The species diffusivity, $D_k$, varies in different subregions of the PEMFC depending on the specific physical phase of component $k$. In flow channels and porous electrodes, species $k$ exists in the gaseous phase, and thus the diffusion coefficient takes the value in gas, whereas species $k$ is dissolved in the membrane phase within the catalyst layers and the membrane, and thus takes the value corresponding to dissolved species, which is usually a few orders of magnitude lower than that in gas. In addition, the diffusion coefficient is a function of temperature and pressure.

$$D(T) = D_0 \left(\frac{T}{T_0}\right)^{3/2} \left(\frac{p_0}{p}\right) \tag{16}$$

The proton conductivity in the membrane phase has been correlated as

$$\sigma_e(T) = 100 \exp\left[1268\left(\frac{1}{303} - \frac{1}{T}\right)\right] \times (0.005139\xi - 0.00326) \tag{17}$$

a reference current density. The stoichiometric ratios inlet streams are given by the following equations.

$$S^{\text{anode}} = C_{H_2} v^{\text{anode}} \frac{2F}{I_{\text{ref}} A} \tag{21}$$

$$S^{\text{cathode}} = C_{O_2} v^{\text{cathode}} \frac{4F}{I_{\text{ref}} A} \tag{22}$$

Water transport through the polymer electrolyte membrane has been investigated by several researchers in different aspects. Most interesting studies in this area includes the determination of water diffusion coefficient and water drag coefficient by Zawodzinski et al. [9, 10] and investigating the diffusion of water in Nafion membranes by Motupally et al. [11].

The electro-osmotic drag coefficient is defined as the number of water molecules transported by each hydrogen proton $H^+$. The electro-osmotic drag coefficient can be expressed with the following equation:

$$n_d = \frac{2.5\xi}{22} \tag{23}$$

The diffusion coefficient of water in Polymer Membrane is also highly dependent on the water content of the membrane. The relation is given as:

$$D_w^m = \begin{Bmatrix} 3.1 \times 10^{-7}\xi(\exp(0.28\xi) - 1)\exp\left(-2346/T\right) & 0 \prec \xi \prec 3 \\ 4.17 \times 10^{-8}\xi(1 + 161\exp(-\xi))\exp\left(-2346/T\right) & \text{otherwise} \end{Bmatrix} \tag{24}$$

where the water content in the membrane, $\xi$, depends on the water activity, $a$, according to the following fit of the experimental data

$$\xi = \begin{cases} 0.043 + 17.18a - 39.85a^2 + 36a^3 & 0 \prec a \leq 1 \\ 14 + 1.4(a-1) & 1 \leq a \leq 3 \end{cases} \tag{18}$$

The water activity is in turn calculated by

$$a = \frac{X_{H_2O} p}{p_{\text{sat}}} \tag{19}$$

where the saturation pressure of water vapor can be computed from the following empirical equation

$$\ln(p^{\text{sat}}) = 70.43464 - \frac{7362.698}{T} + 0.006952T - 9\ln(T) \tag{20}$$

In a fuel cell system, the inlet flow rates are generally expressed as stoichiometric ratios of inlet streams based on

Once the electrolyte phase potential is determined in the membrane, the local current density along the axial direction can be calculated as follows

$$I(y) = -\sigma_e^{\text{eff}} \left.\frac{\partial \phi_e}{\partial x}\right|_{x=\text{I.F.}} \tag{25}$$

where I.F. means the interface between the membrane and cathode catalyst layer. The average current density is then determined by

$$I_{\text{avg}} = \frac{1}{L}\int_0^L I(y)\mathrm{d}y \tag{26}$$

where $L$ is the cell length.

There are natural boundary conditions of zero-flux prescribed everywhere other than the inlet and outlets of the flow channels. The boundary conditions prescribed at the inlets of the gas channels are:

| | |
|---|---|
| $u_{\text{in}}^{\text{anode}} = u_a^0$ | $u_{\text{in}}^{\text{cathode}} = u_c^0$ |
| $C_{H_2}^{\text{anode,in}} = C_{H_2}^0$ | $C_{O_2}^{\text{cathode,in}} = C_{O_2}^0$ |
| $C_{H_2O}^{\text{anode,in}} = C_{H_2O}^{0,a}$ | $C_{H_2O}^{\text{cathode,in}} = C_{H_2O}^{0,c}$ |

A mesh with 498,592 nodes was found to provide required spatial resolution for different channel geometry. The solution is considered to be converged when the difference between successive iterations is $<10^{-7}$ for all variables.

The Electrochemical and Transport Parameters used in these simulations are summarized in Table 2, and the operational parameters are presented in Table 3.

## 3 Results and discussion

In order to show that the program in this study can handle the cell performance of a PEMFC, we apply the present method to solve the whole of a PEMFC as described in Miansari et al. [12]. The physical parameters and properties of the fuel cell are listed in Fig. 2. The mesh employed for the comparison with the reference was 241 × 74 × 25. The steady-state solution is obtained by the numerical procedure as mentioned in the previous section. As shown in Fig. 2, the result of the present predictions of the polarization curve agreeing fairly closely with Miansari et al. [12] gives one confidence in the use of the present program.

Figure 3 shows the polarization curves with two GDL porosity of a duct-shaped fuel cell at cell voltage of 0.4 V

**Table 2** Electrochemical and transport properties

| Description | Unit | Value |
|---|---|---|
| Anode reference exchange current density | $A/m^3$ | 1.5e9 |
| Cathode reference exchange current density | $A/m^3$ | 4,000,000 |
| Anode transfer coefficient | | 2 |
| Cathode transfer coefficient | | 2 |
| Faraday constant | C/mol | 96,487 |
| $H_2$ diffusivity | $m^2/s$ | 3e−5 |
| $O_2$ diffusivity | $m^2/s$ | 3e−5 |
| $H_2O$ diffusivity at anode | $m^2/s$ | 3e−5 |
| $H_2O$ diffusivity at cathode | $m^2/s$ | 3e−5 |
| Anode backing layer porosity | | 0.5 |
| Cathode backing layer porosity | | 0.5 |
| Permeability of anode backing layer | $m^2$ | e−12 |
| Permeability of cathode backing layer | $m^2$ | e−12 |
| Equivalent weight of membrane | kg/mol | 1.1 |

**Table 3** Operational parameters

| Description | Unit | Value |
|---|---|---|
| Reference average current density | $A/cm^2$ | 1.0 |
| Anode inlet velocity | m/s | 0.5 |
| Cathode inlet velocity | m/s | 1 |
| Anode inlet pressure | Atm | 1 |
| Cathode inlet pressure | Atm | 1 |
| Cell temperature | °C | 70 |
| Anode inlet molar concentration | | |
| Hydrogen | $mol/m^3$ | 35.667 |
| Oxygen | $mol/m^3$ | 0 |
| Water vapor | $mol/m^3$ | 16.121 |
| Cathode inlet molar concentration | | |
| Hydrogen | $mol/m^3$ | 0 |
| Oxygen | $mol/m^3$ | 7.51 |
| Water vapor | $mol/m^3$ | 16.121 |

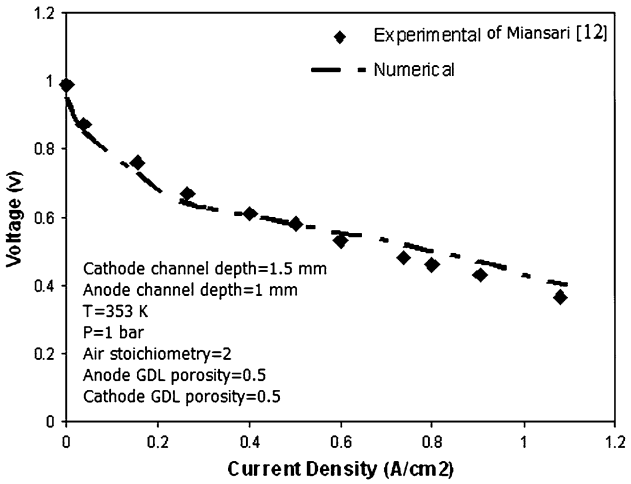


**Fig. 2** Comparison between results of this paper and results of Miansari et al. [12]

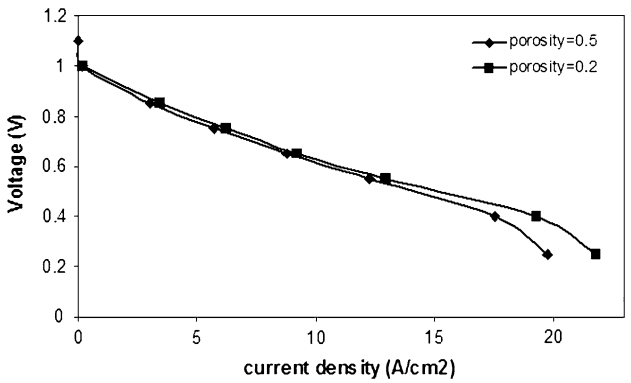


**Fig. 3** Effect of GDL porosity on variation of cell performance

to investigate the influence of GDL porosity on the cell performance. It shows in Fig. 3 that the effect of the GDL porosity on the cell performance is significant at high

current density. However, at low current density, the influence of GDL porosity on the polarization curve is negligibly small. It is also observed that the cell performance is increased as the GDL porosity decreases that it is clear there is difference between duct-shaped and planner fuel cell. This is due to that the porosity of the gas diffusion layer has two comparing effects on the fuel cell performance; (1) an increase in the porosity provides the space for the reactants to diffuse towards the catalyst region and means that the onset of mass transport limitations occurs at higher current densities that it leads to higher limiting currents and (2) the adverse effect of a high porosity is an expected increase in the contact resistance. Therefore, a GDL material having lower porosity is strongly recommended for duct-shaped fuel cells designed to operate with high power.

Figure 4 shows the effect of GDL thermal conductivity on the performance of a duct-shaped PEM fuel cell at cell voltage of 0.4 V. The heat produced by the electrochemical reaction at the cathode side catalyst layer can dry the membrane and decrease the transportation of proton from it. Therefore in order to prevent drying out of the membrane and excessive thermal stresses it is required to remove the heat produced at the catalyst layer through the gas diffusion layer that this is controlled by the GDL thermal conductivity. It is clear from Fig. 4 that the effect of the GDL thermal conductivity on the cell performance is significant at high current density but at low current density, the influence of GDL thermal conductivity on the polarization curve is negligibly small. Also it is clear that by increasing the thermal conductivity of the GDL the overall cell performance increases that this is due to increasing the lateral conduction of heat produced at the cathode catalyst layer. Therefore, a GDL material having higher thermal conductivity is strongly recommended for duct-shaped fuel cells designed to operate with high power.

The effect of gas diffusion layer thickness on the duct-shaped fuel cell performance at cell voltage of 0.4 V is shown in Fig. 5. It is obvious that a thinner gas diffusion layer increases the mass transport through it, and this leads to reduction the mass transport loss but for a duct-shaped fuel cell there is a little difference because that the effect of changing the surface overcome the effect of thickness of the layer that by decreasing the thickness of the GDL the surface of the cell at the catalyst layer decreases. Also in Fig. 5 it is clear that by increasing the gas diffusion layer thickness the overall cell performance increases. Also the molar oxygen fraction at the catalyst layer increases with a decreasing of the gas diffusion layer thickness due to the reduced resistance to the oxygen diffusion by the thinner layer. Therefore, a GDL material having higher thickness is strongly recommended for duct-shaped fuel cells designed to operate with high power.

The maximum temperature with higher gradient appears in the cathode side catalyst layer of the fuel cell. The higher membrane conductivity results in more even distribution of the temperature in the cell, due to the removal of cathode waste heat to the anode gas diffusion layer and then to the anode gas stream through the membrane. In Fig. 6 the

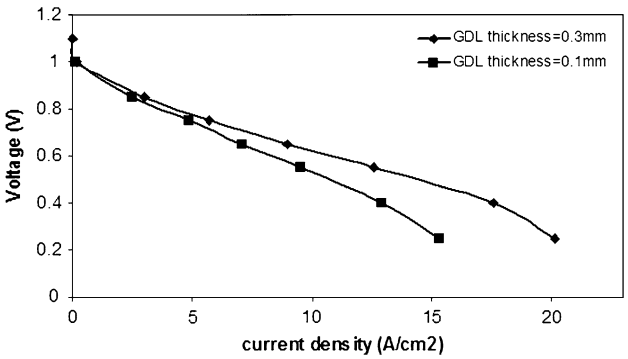


**Fig. 5** Effect of GDL thickness on variation of cell performance

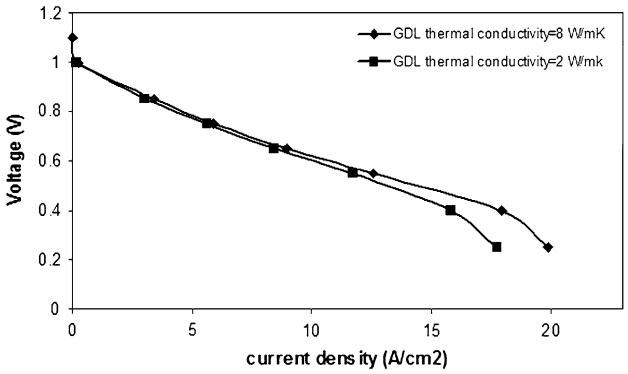


**Fig. 4** Effect of GDL thermal conductivity on variation of cell performance

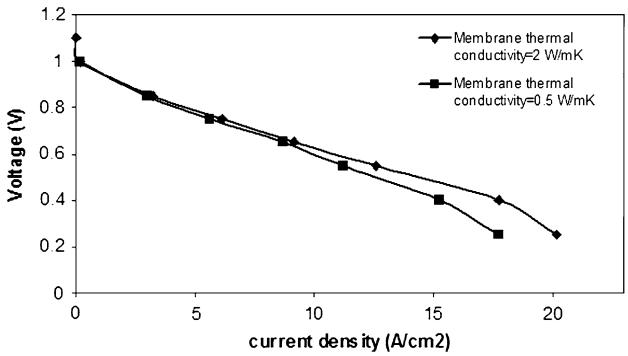


**Fig. 6** Effect of membrane thermal conductivity on variation of cell performance

effect of membrane thermal conductivity on the performance of a duct-shaped PEM fuel cell at cell voltage of 0.4 V are shown. It is clear from Fig. 6 that the effect of the membrane thermal conductivity on the cell performance is significant at high current density but at low current density, the influence of membrane thermal conductivity on the polarization curve is negligibly small. Also Fig. 6 shows that by increasing the thermal conductivity of the membrane the overall cell performance increases that this is due to increasing the lateral conduction of heat produced at the cathode catalyst layer to the anode gas diffusion layer. Therefore, a membrane material having higher thermal conductivity is strongly recommended for duct-shaped fuel cells designed to operate with high power.

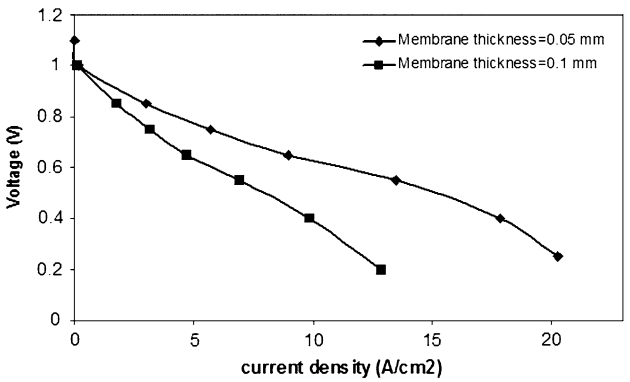


**Fig. 7** Effect of membrane thickness on variation of cell performance

Figure 7 shows the effect of membrane thickness on the performance of a duct-shaped PEM fuel cell at cell voltage of 0.4 V. The effect of membrane thickness on the fuel cell performance is mostly on the resistance of the proton transport across the membrane. The potential loss in the membrane is due to resistance to proton transport across the membrane from anode catalyst layer to cathode catalyst layer. Therefore, a reduction in the membrane thickness means that the path traveled by the protons will be decreased; thereby reducing the membrane thickness leads to reduce the membrane resistance and this leads to enhance the overall cell performance as can be shown in Fig. 7. Therefore, a membrane material having lower thickness is strongly recommended for duct-shaped fuel cells designed to operate with high power.

Figure 8 shows the ability of the model that is used in this research that is a full fuel cell model, which includes all the parts of the PEM fuel cell, flow channels, gas diffusion electrodes, catalyst layers and the membrane. The local current density distribution at the cathode side catalyst layer for two different GDL thickness (a) $t_{GDL} = 0.3$ mm and (b) $t_{GDL} = 0.1$ mm at 0.4 V cell voltage. It can be seen that for a low GDL thickness, the distribution is quite uniform. It is clear that the current density is higher at the connections between GDL and bipolar plate that these peak regions of the distribution of the local current density are caused by the transverse installation of the connections. Also it is clear that the maximum of local current density decreased and the distribution of the current density can be uniform by decreasing the GDL thickness.

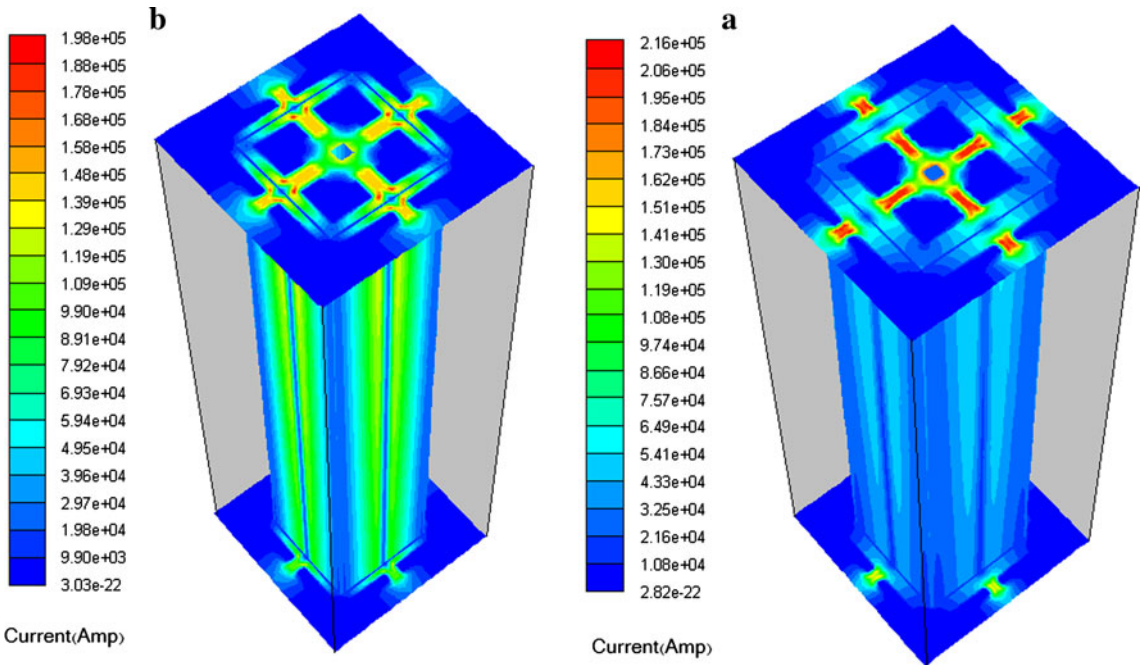


**Fig. 8** Local current density distribution at cathode side catalyst layer for two different GDL thicknesses: **a** 0.3 mm and **b** 0.1 mm

## 4 Conclusion

A complete 3-dimensional and single phase model for duct-shaped proton exchange membrane (PEM) fuel cell was used to investigate the effect of changing gas diffusion layer and membrane properties on the performances, current density and gas concentration. The complete 3-dimensional model for PEM fuel cells based on the two-fluid method was numerically solved with constant-temperature boundary condition at surfaces of anode and cathode current collectors. The results of this paper are in good agreement with experimental results of Miansari et al. [12]. The results show that the effect of the GDL porosity on the cell performance is significant at high current density and the cell performance is increased as the GDL porosity decreases and the gas diffusion layer thickness increases that this is different with planner fuel cell. Also the results show that by increasing the thermal conductivity of the membrane the overall cell performance increases that this is due to increasing the lateral conduction of heat produced at the cathode catalyst layer to the anode gas diffusion layer. The model is shown in this study to be able to: (1) understand the effect of changing properties of the materials; (2) create a numerical method of optimization of a duct-shaped PEM fuel cell.

**Acknowledgments** This work was partially supported by Renewable Energy Organization of Iran.

## References

1. Larminie J, Dicks A (2003) Fuel cell system explained, 2nd edn. Wiley, New Jersey
2. Khazaee I, Ghazikhani M (2011) Performance improvement of proton exchange membrane fuel cell by using annular shaped geometry. J Power Sources 196:2661–2668
3. West AC, Fuller TF (1996) The influence of rib spacing in proton-exchange membrane electrode assemblies. J Appl Electrochem 26:557–565
4. Chiang MS, Chu HS (2006) Transient behavior of CO poisoning of the anode catalyst layer of a PEM fuel cell. J Power Sources 160:340–352
5. Wang ZH, Wang CY, Chen KS (2001) Two-phase flow and transport in the air cathode of proton exchange membrane fuel cells. J Power Sources 94:40–50
6. Kuo JK, Yen TS, Chen CK (2008) Improvement of performance of gas flow channel in PEM fuel cells. Energy Convers Manag 49:2776–2787
7. Yan WM, Soong CY, Chen FL, Chu HS (2004) Effects of flow distributor geometry and diffusion layer porosity on reactant gas transport and performance of PEM fuel cells. J Power Sources 125:27–39
8. Chu HS, Yeh C, Chen F (2003) Effects of porosity change of gas diffuser on performance of proton exchange membrane fuel cell. J Power Sources 123:1–9
9. Zawodzinski TA, Neeman JM, Sillerud LO, Gottesfeld S (1991) Determination of water diffusion coefficients in perfluorosulfonate ionomeric membranes. J Phys Chem 95:6040–6044
10. Zawodzinski TA, Davey J, Valerio J, Gottesfeld S (1995) The water content dependence of electro-osmotic drag in proton-conducting polymer electrolytes. Electrochim Acta 40:297–302
11. Motupally S, Becker AJ, Weidner JW (2000) Diffusion of water through nafion® 115 membranes. J Electrochem Soc 147:3171–3177
12. Miansari Me, Sedighi K, Amidpour M, Alizadeh E, Miansari Mo (2009) Experimental and thermodynamic approach on proton exchange membrane fuel cell performance. J Power Sources 190:356–361